

## Supplementary Material

### **A systematic assessment of the metallome of selected plant families in the Queensland (Australia) flora by using X-ray fluorescence spectroscopy**

*Imam Purwadi<sup>A</sup>, Farida Abubakari<sup>A</sup>, Gillian K. Brown<sup>B</sup>, Peter D. Erskine<sup>A</sup>, and Antony van der Ent<sup>A,C,\*</sup>*

<sup>A</sup>Centre for Mined Land Rehabilitation, Sustainable Minerals Institute, The University of Queensland, Brisbane, Qld 4072, Australia.

<sup>B</sup>Department of Environment and Science, Queensland Herbarium, Toowong, Qld 4066, Australia.

<sup>C</sup>Laboratory of Genetics, Wageningen University and Research, The Netherlands; and Laboratoire Sols et Environnement, INRAE, Université de Lorraine, France.

\*Correspondence to: Antony van der Ent, Centre for Mined Land Rehabilitation, Sustainable Minerals Institute, The University of Queensland, Brisbane, Qld 4072, Australia; Email: [a.vanderent@uq.edu.au](mailto:a.vanderent@uq.edu.au)

This supplementary information is to provide information how the accuracy of empirical calibrations used to correct Mn concentrations in the previous studies (Abubakari et al. 2021a, b, c) is compared to GeoPIXE used in this study. The empirical formula is  $y = 0.7869x^{0.9165}$  where  $y$  is the corrected Mn concentrations, and  $x$  is the Mn concentration reported by the portable XRF instrument. The formula was not written in the articles and obtained by contacting the corresponding author of the articles (Abubakari et al. 2021a, b, c). Manganese concentrations of 588 disc leaves provided by Purwadi et al. (2021a) is used to assess the accuracy of both approach. Out of 588-disc leaves, only 333-disc leaves with Mn concentration more than the limit of detection (Table S2). The  $R^2$  value of empirical calibration (0.59) is slightly higher than that of GeoPIXE (0.55) as shown in Figure S3, but the root mean square error of the empirical calibration approach (6112) is 16% more than that of GeoPIXE (5290).

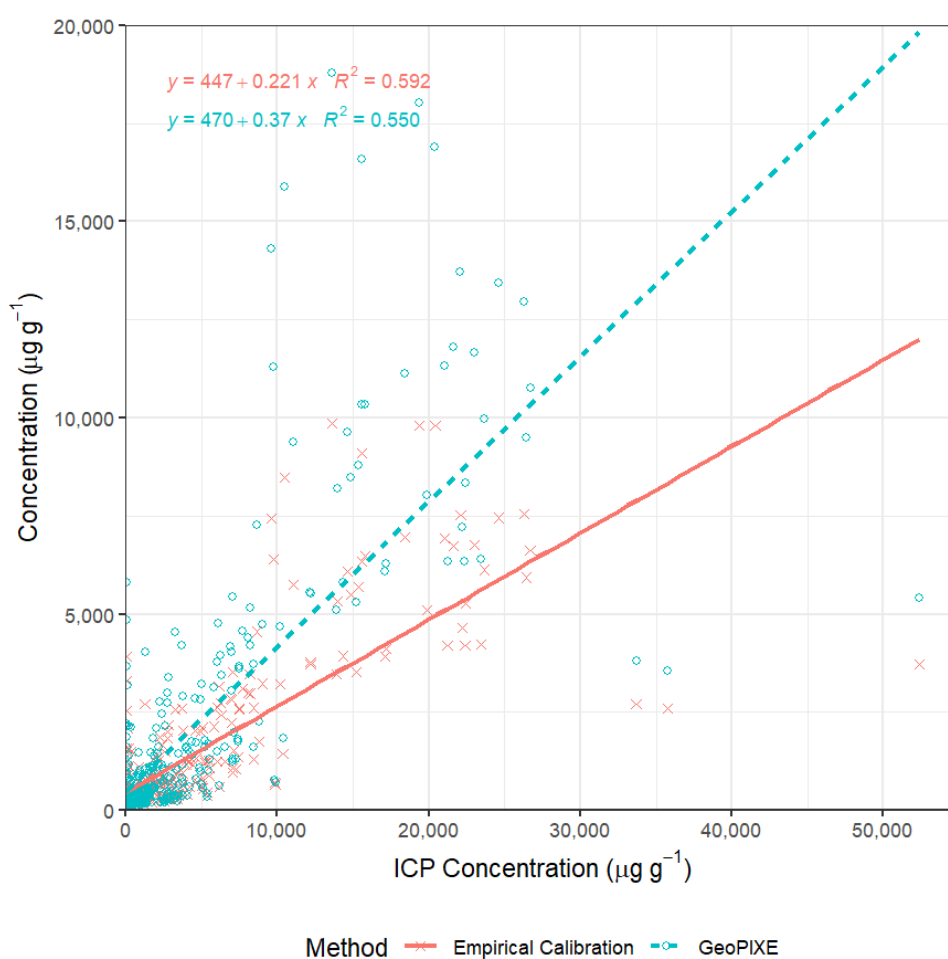


**Figure S1.** A scatter plot comparing Mn concentrations corrected using Empirical Calibration and GeoPIXE plotted against Mn concentrations obtained from ICP Analysis.

Manganese concentration ( $\mu\text{g g}^{-1}$ )  
Hyperaccumulator threshold  $> 10\,000 \mu\text{g g}^{-1}$

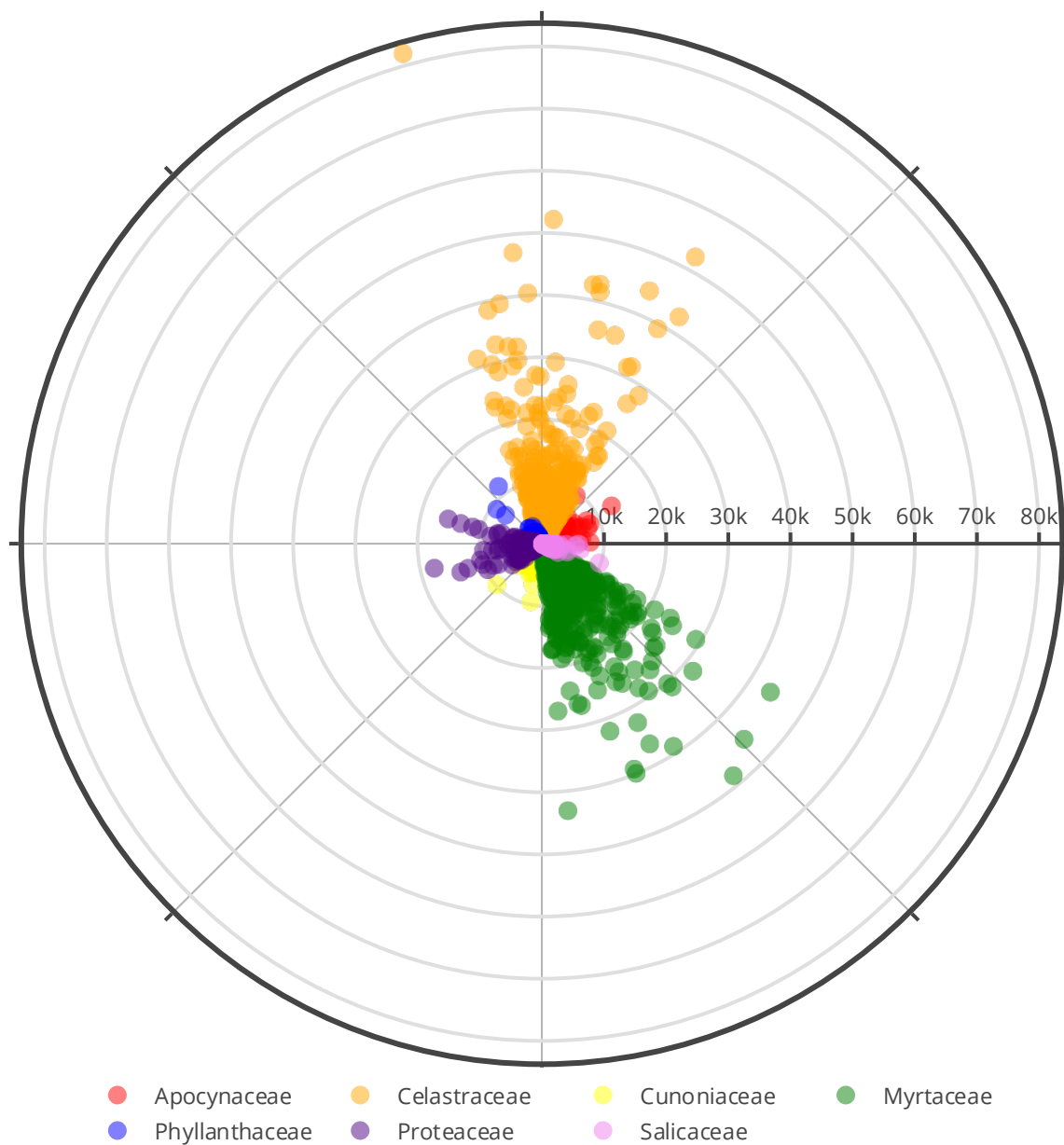


**Figure S2.** Manganese concentrations detected in the specimens across seven families: Apocynaceae (red), Celastraceae (orange), Cunoniaceae (yellow), Myrtaceae (green), Phyllanthaceae (blue), Proteaceae (indigo), and Salicaceae (violet). The far points from the centre of the circle, the higher concentration. The notional threshold of manganese hyperaccumulator plants is  $10\,000 \mu\text{g g}^{-1}$ .

Cobalt concentration ( $\mu\text{g g}^{-1}$ )  
Hyperaccumulator threshold  $> 300 \mu\text{g g}^{-1}$

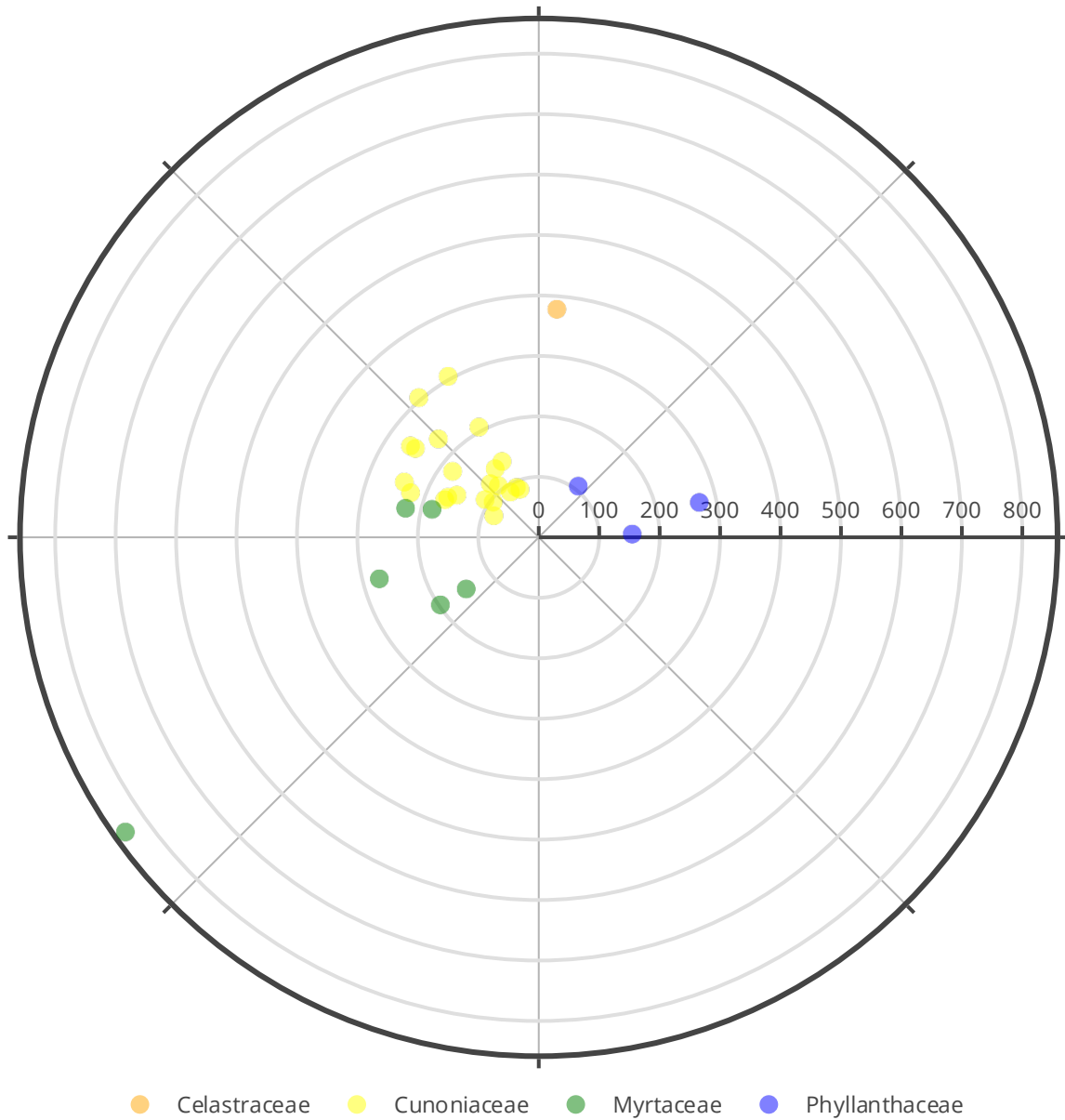


**Figure S3.** Cobalt concentrations detected in the specimens across seven families: Celastraceae (orange), Cunoniaceae (yellow), Myrtaceae (green), and Phyllanthaceae (blue). The far points from the centre of the circle, the higher concentration. The notional threshold of cobalt hyperaccumulator plants is  $300 \mu\text{g g}^{-1}$ .

Nickel concentration ( $\mu\text{g g}^{-1}$ )  
Hyperaccumulator threshold  $> 1\,000\ \mu\text{g g}^{-1}$

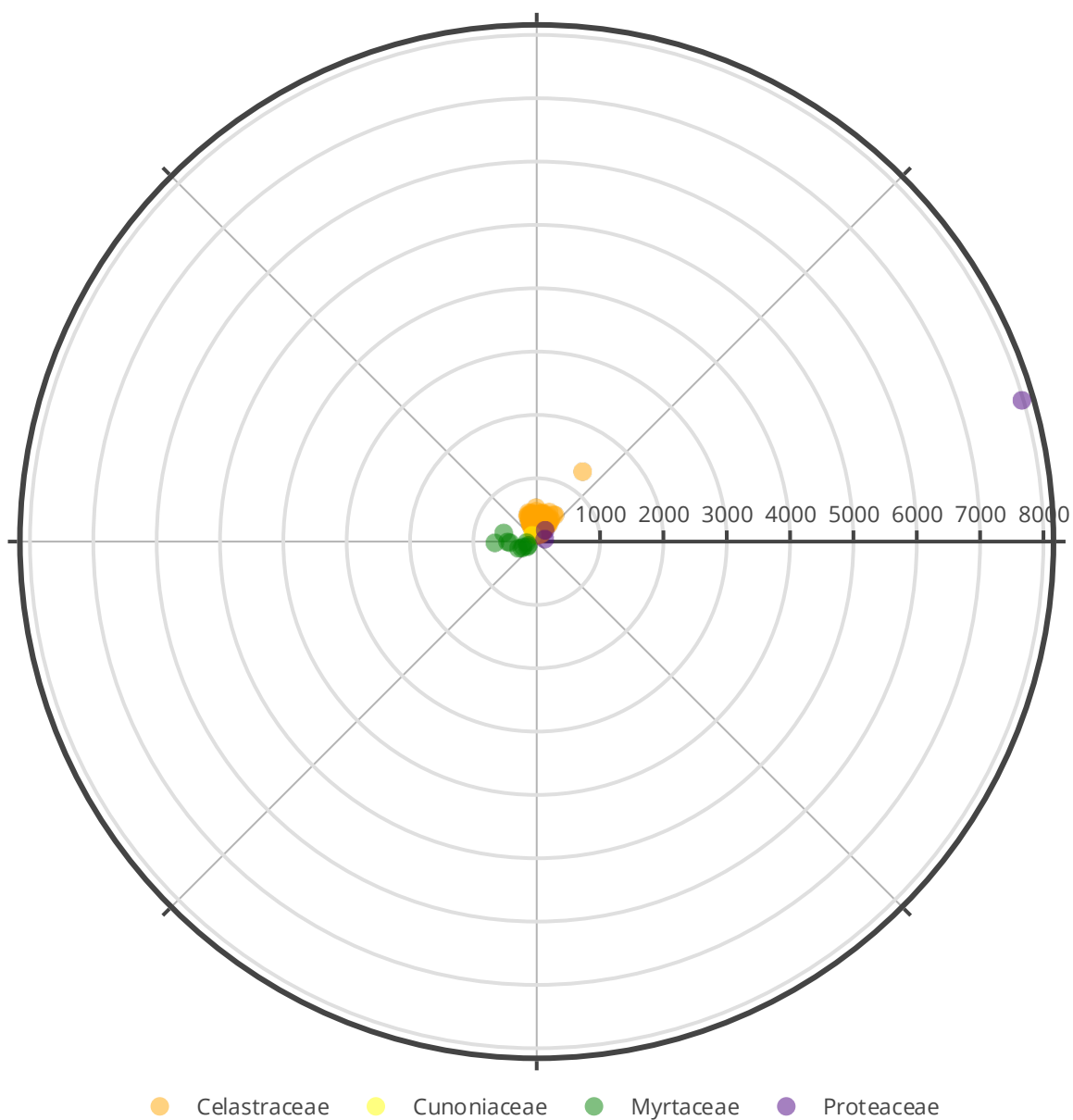


**Figure S4.** Nickel concentrations detected in the specimens across seven families: Celastraceae (orange), Cunoniaceae (yellow), Myrtaceae (green), and Proteaceae (indigo). The far points from the centre of the circle, the higher concentration. The notional threshold of nickel hyperaccumulator plants is  $1000\ \mu\text{g g}^{-1}$ .

Zinc concentration ( $\mu\text{g g}^{-1}$ )  
Hyperaccumulator threshold  $> 3\,000\ \mu\text{g g}^{-1}$

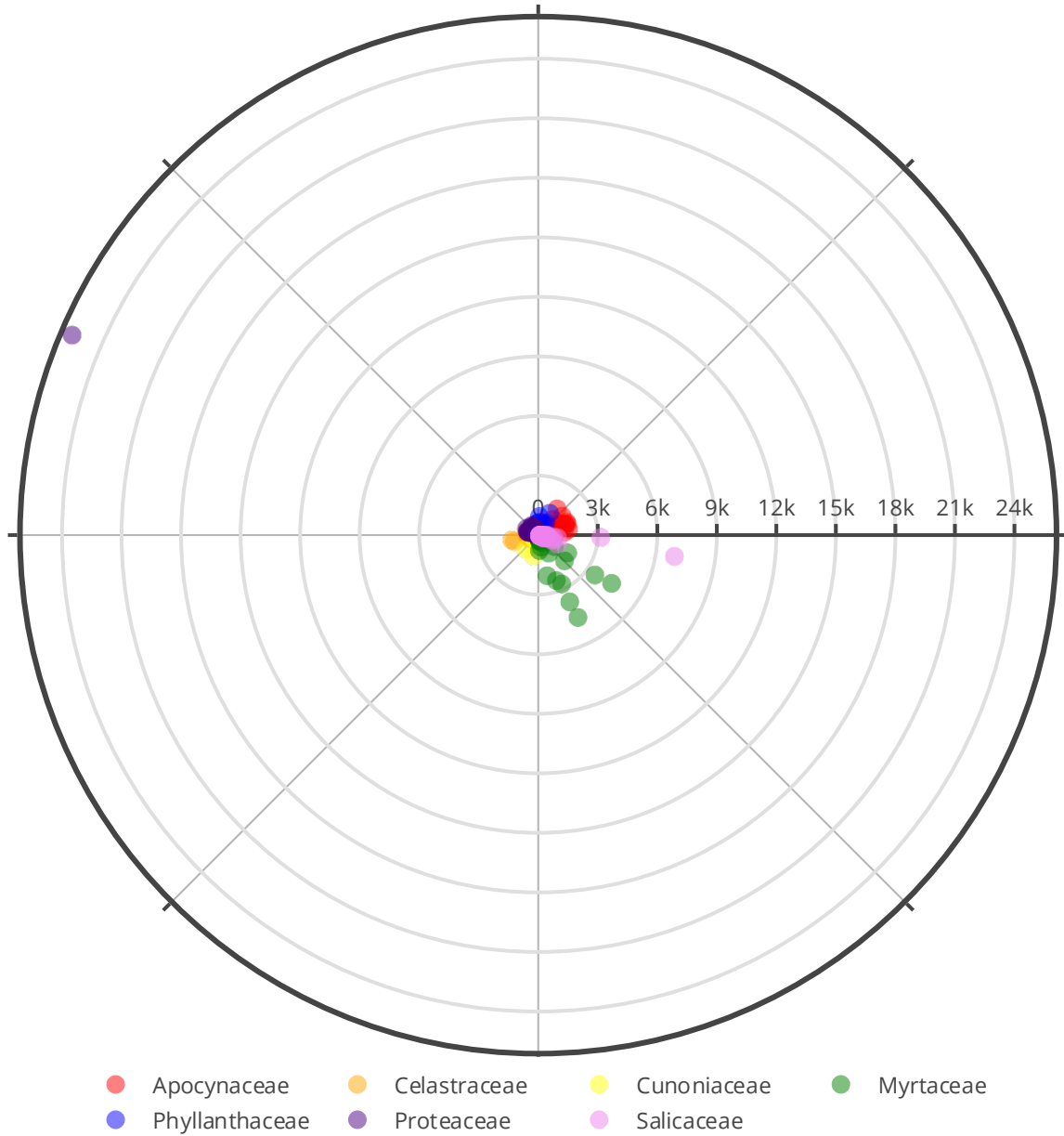


**Figure S5.** Zinc concentrations detected in the specimens across seven families: Apocynaceae (red), Celastraceae (orange), Cunoniaceae (yellow), Myrtaceae (green), Phyllanthaceae (blue), Proteaceae (indigo), and Salicaceae (violet). The far points from the centre of the circle, the higher concentration. The notional threshold of zinc hyperaccumulator plants is  $3000\ \mu\text{g g}^{-1}$ .

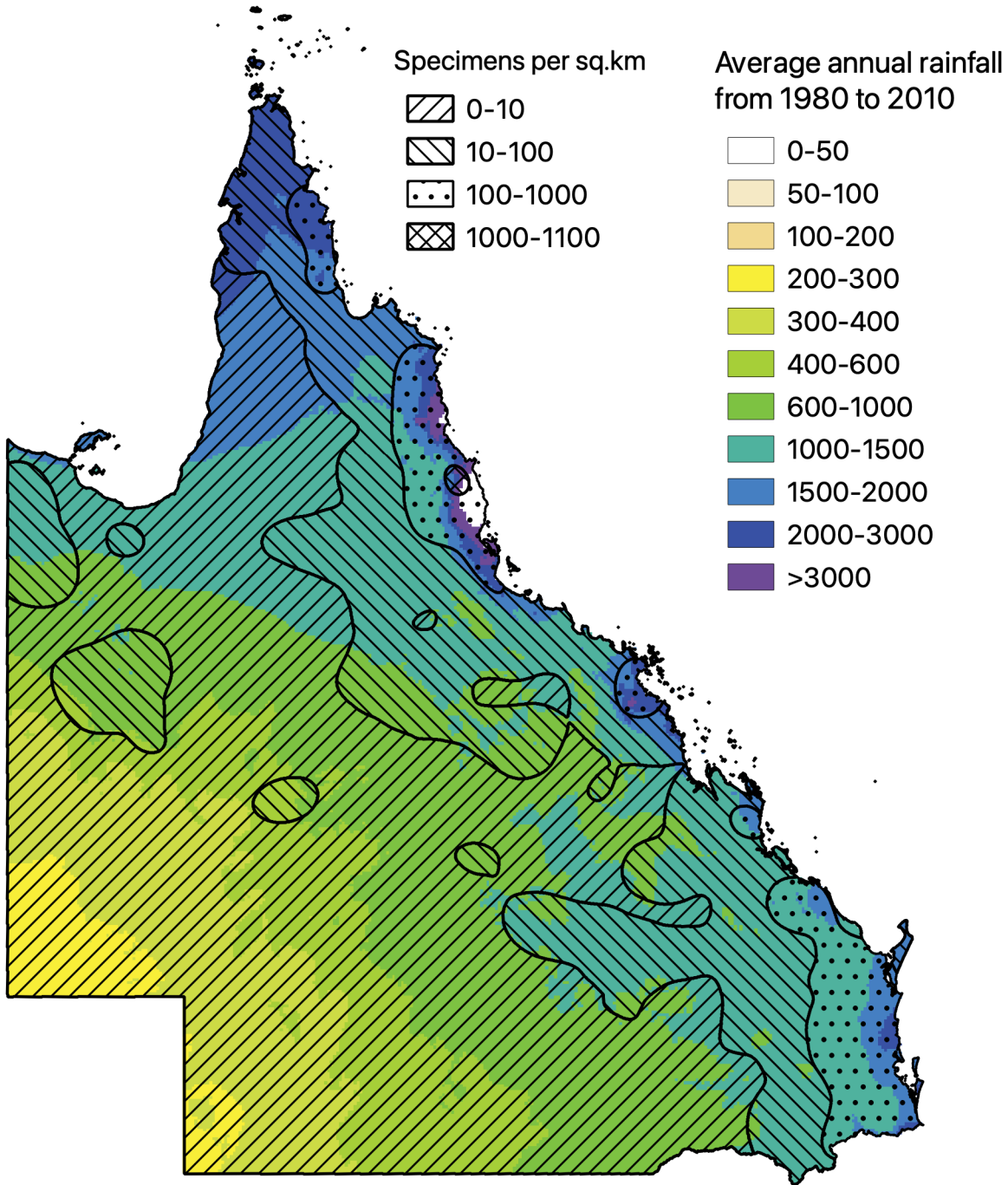


**Figure S6.** Map showing the number of specimens taken per one square kilometre on top of Queensland average annual rainfall from 1980 to 2010 (Australian Bureau of Meteorology 2020).

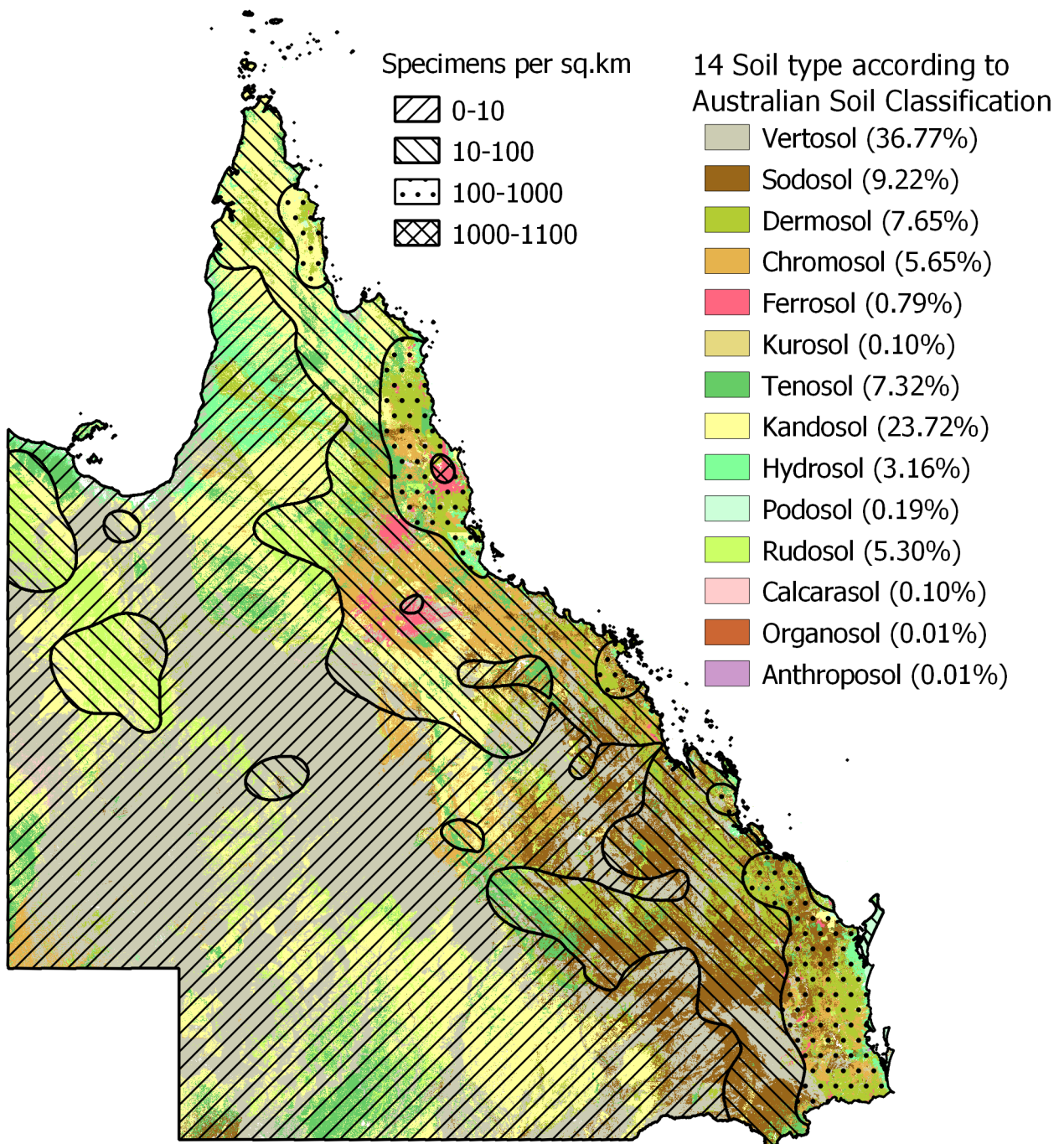


**Figure S7.** Map showing the number of specimens taken per one square kilometre on top of 14 soil types (Searle 2021).

Table S1 shows the results of processing three pure thin film standards (titanium, gold, and tin). The three were chosen because the fluorescent lines of the three covers low to high energy (4.5KeV to 25KeV). By processing the raw spectra in the proposed pipeline, the maximum errors are only 4%.

**Table S1.** The reported concentration of three pure thin films by the proposed algorithm

<b>Element</b>	<b>Titanium</b>	<b>Gold</b>		<b>Tin</b>	
Fluorescence line	K	L	M	K	L
Concentration	104%	98%	98%	100%	98%

**Table S2.** Root mean square error calculation for Empirical Calibration and GeoPIXE approach.

<b>Mn Concentration (<math>\mu\text{g g}^{-1}</math>)</b>				<b>Error</b>	
<b>ICP</b>	<b>XRF</b>	<b>Empirical Calibration</b>	<b>GeoPIXE</b>	<b>XRF</b>	<b>GeoPIXE</b>
807	341	165	128	642	679
562	350	169	131	393	431
174	299	146	132	28	42
523	349	168	133	355	390
202	322	156	134	46	68
1111	350	169	140	942	971
366	374	179	141	187	225
214	399	190	142	24	72
207	357	172	143	35	64
19	371	178	143	-159	-124
405	443	210	147	195	258
42	430	204	150	-162	-108
297	444	210	152	87	145
445	436	207	152	238	293
226	413	197	154	29	72
293	457	216	158	77	135
1081	407	194	158	887	923
869	398	190	159	679	710
246	449	212	160	34	86
107	419	199	160	-92	-53
236	444	210	162	26	74
133	335	162	162	-29	-29
1379	506	237	163	1142	1216
584	402	192	167	392	417
299	453	214	174	85	125
396	267	132	176	264	220
350	443	210	179	140	171
1118	441	209	180	909	938
7	359	173	181	-166	-174
1189	475	223	182	966	1007
787	470	221	182	566	605
691	390	187	182	504	509
610	399	190	182	420	428
291	546	254	184	37	107
253	456	215	187	38	66
50	478	225	187	-175	-137
1710	449	212	196	1498	1514
554	533	248	198	306	356

Mn Concentration ( $\mu\text{g g}^{-1}$ )				Error	
ICP	XRF	Empirical Calibration	GeoPIXE	XRF	GeoPIXE
509	482	226	198	283	311
902	575	266	201	636	701
736	449	212	202	524	534
802	479	225	202	577	600
1124	541	252	203	872	921
508	398	190	206	318	302
347	483	227	207	120	140
169	423	201	207	-32	-38
2294	615	283	207	2011	2087
239	477	224	208	15	31
359	525	245	209	114	150
2502	524	245	209	2257	2293
1269	572	265	212	1004	1057
210	495	232	213	-22	-3
2583	594	274	214	2309	2369
259	549	255	215	4	44
751	582	269	218	482	533
958	534	249	218	709	740
465	611	281	219	184	246
763	460	217	221	546	542
383	576	267	226	116	157
53	601	277	230	-224	-177
259	429	203	230	56	29
448	576	267	231	181	217
918	518	242	235	676	683
560	684	312	237	248	323
3441	635	292	238	3149	3203
301	577	267	243	34	58
478	564	261	246	217	232
1072	539	251	247	821	825
867	595	275	249	592	618
401	675	308	250	93	151
1065	548	255	250	810	815
2563	661	302	252	2261	2311
689	535	249	254	440	435
1278	579	268	255	1010	1023
1137	609	281	257	856	880
2734	659	302	257	2432	2477
201	525	245	260	-44	-59
54	608	280	261	-226	-207

Mn Concentration ( $\mu\text{g g}^{-1}$ )				Error	
ICP	XRF	Empirical Calibration	GeoPIXE	XRF	GeoPIXE
581	562	261	262	320	319
2598	662	303	263	2295	2335
233	546	254	265	-21	-32
487	554	257	270	230	217
931	580	268	270	663	661
2952	685	313	270	2639	2682
726	753	341	271	385	455
3170	715	325	272	2845	2898
180	539	251	280	-71	-100
280	639	293	281	-13	-1
280	635	292	285	-12	-5
358	632	290	290	68	68
470	676	309	290	161	180
253	632	290	293	-37	-40
2841	685	312	296	2529	2545
942	614	283	303	659	639
2740	779	352	304	2388	2436
7	678	310	307	-303	-300
1602	699	318	311	1284	1291
451	693	316	314	135	137
864	811	365	316	499	548
976	710	323	316	653	660
978	736	334	318	644	660
1222	656	301	319	921	903
917	620	285	321	632	596
768	639	293	322	475	446
1138	788	355	332	783	806
1283	677	309	339	974	944
765	832	373	352	392	413
3481	850	381	352	3100	3129
5381	834	374	355	5007	5026
1330	734	333	366	997	964
1375	829	372	369	1003	1006
414	755	342	370	72	44
1535	795	358	371	1177	1164
3774	897	400	371	3373	3403
3239	887	396	374	2843	2865
4033	876	392	375	3641	3658
1059	819	368	378	691	681
1075	823	370	379	705	696

Mn Concentration ( $\mu\text{g g}^{-1}$ )				Error	
ICP	XRF	Empirical Calibration	GeoPIXE	XRF	GeoPIXE
3189	860	385	381	2804	2808
1999	824	370	384	1629	1615
2433	812	365	385	2068	2048
62	843	378	387	-316	-325
804	868	388	388	416	416
1319	825	371	395	948	924
1037	844	378	395	659	642
1468	901	402	398	1066	1070
1430	916	408	400	1022	1030
312	725	329	403	-17	-91
433	837	375	405	58	28
1565	830	372	408	1193	1157
3454	978	433	416	3021	3038
2793	1019	450	422	2343	2371
848	812	365	423	483	425
1596	967	429	432	1167	1164
5390	1033	455	437	4935	4953
1409	948	421	443	988	966
14	637	292	445	-278	-431
179	985	436	447	-257	-268
134	962	427	448	-293	-314
1198	965	428	451	770	747
1477	1002	443	455	1034	1022
1606	923	411	465	1195	1141
2683	1073	472	465	2211	2218
749	1066	469	471	280	278
1207	949	421	472	786	735
495	896	400	473	95	22
847	973	431	475	416	372
3011	1129	494	495	2517	2516
1134	1077	473	498	661	636
701	1018	449	517	252	184
1908	1189	518	526	1390	1382
548	1109	486	535	62	13
1319	1099	482	537	837	782
1536	1120	490	537	1046	999
1150	1169	510	541	640	609
511	1022	451	548	60	-37
1940	1216	529	560	1411	1380
1776	1140	498	563	1278	1213

Mn Concentration ( $\mu\text{g g}^{-1}$ )				Error	
ICP	XRF	Empirical Calibration	GeoPIXE	XRF	GeoPIXE
5099	1276	553	572	4546	4527
1740	1139	498	573	1242	1167
1868	1199	522	576	1346	1292
793	1201	523	578	270	215
183	1340	578	594	-395	-411
3030	1206	525	597	2505	2433
4224	1362	587	607	3637	3617
186	1227	533	609	-347	-423
1637	1199	522	614	1115	1023
6165	1383	595	623	5570	5542
1015	1167	509	636	506	379
2554	1264	548	637	2006	1917
1480	1296	561	642	919	838
3579	1396	600	643	2979	2936
1728	1375	592	651	1136	1077
451	1262	547	665	-96	-214
4989	1460	625	665	4364	4324
773	1307	565	676	208	97
1932	1532	653	701	1279	1231
3739	1528	652	702	3087	3037
1578	1473	630	704	948	874
9860	1566	667	707	9193	9153
259	1512	646	717	-387	-458
2484	1593	677	742	1807	1742
366	1255	544	751	-178	-385
9791	1672	708	765	9083	9026
1192	1609	683	780	509	412
4682	1719	726	798	3956	3884
2286	1541	657	809	1629	1477
2994	1636	694	811	2300	2183
2259	1735	732	813	1527	1446
110	1488	636	816	-526	-706
3698	1555	662	824	3036	2874
2797	1668	706	839	2091	1958
705	1507	644	850	61	-145
895	1783	751	863	144	32
1275	1700	719	883	556	392
504	1729	730	896	-226	-392
886	1770	746	932	140	-46
1899	1905	798	941	1101	958

Mn Concentration ( $\mu\text{g g}^{-1}$ )				Error	
ICP	XRF	Empirical Calibration	GeoPIXE	XRF	GeoPIXE
45	1690	715	942	-670	-897
2115	1806	760	995	1355	1120
4974	1882	789	1000	4185	3974
1564	2064	859	1004	705	560
5485	2123	881	1022	4604	4463
899	1803	759	1027	140	-128
1267	1886	791	1033	476	234
2526	2087	867	1042	1659	1484
2456	2014	840	1047	1616	1409
3318	2147	890	1056	2428	2262
2485	1860	780	1059	1705	1426
1652	2055	855	1065	797	587
4837	2185	905	1069	3932	3768
1814	2172	900	1078	914	736
3030	1944	813	1101	2217	1929
1567	2177	902	1112	665	455
41	2260	933	1114	-892	-1073
1805	2211	915	1133	890	672
3803	2294	946	1160	2857	2643
2412	2053	854	1162	1558	1250
207	2067	860	1167	-653	-960
2177	2287	943	1174	1234	1003
7081	2366	973	1231	6108	5850
20	2507	1026	1300	-1006	-1280
5487	2655	1082	1305	4405	4182
7061	2609	1064	1305	5997	5756
7277	2562	1047	1306	6230	5971
1910	2689	1094	1388	816	522
168	2794	1133	1391	-965	-1223
4449	2854	1156	1411	3293	3038
2072	2730	1110	1437	962	635
3451	2371	975	1437	2476	2014
886	2709	1102	1458	-216	-572
1626	2628	1072	1477	554	149
6013	3072	1237	1509	4776	4504
4161	3066	1234	1522	2927	2639
4001	3184	1278	1569	2723	2432
4018	2886	1168	1597	2850	2421
8461	3237	1297	1598	7164	6863
2149	3176	1275	1611	874	538

Mn Concentration ( $\mu\text{g g}^{-1}$ )				Error	
ICP	XRF	Empirical Calibration	GeoPIXE	XRF	GeoPIXE
30	2411	990	1619	-960	-1589
6528	3113	1252	1620	5276	4908
5205	3039	1224	1623	3981	3582
5473	3135	1259	1699	4214	3774
4653	3308	1323	1730	3330	2923
7422	3416	1363	1745	6059	5677
4369	3250	1302	1746	3067	2623
5227	3175	1274	1782	3953	3445
7397	3372	1346	1797	6051	5600
1821	3274	1311	1822	510	-1
10369	3616	1436	1827	8933	8542
50	3145	1263	1851	-1213	-1801
7102	3868	1527	1976	5575	5126
1996	3524	1402	2099	594	-103
371	3807	1505	2102	-1134	-1731
227	4016	1581	2152	-1354	-1925
2573	3815	1508	2152	1065	421
32	3783	1496	2157	-1464	-2125
34	4006	1577	2194	-1543	-2160
8799	4471	1744	2269	7055	6530
2398	4285	1677	2443	721	-45
2784	4755	1845	2746	939	38
2259	4829	1871	2761	388	-502
4923	5198	2002	2826	2921	2097
4575	5270	2028	2851	2547	1724
3774	5278	2030	2904	1744	870
2758	5174	1994	3003	764	-245
6964	5812	2218	3055	4746	3909
5832	5556	2128	3132	3704	2700
129	5460	2094	3172	-1965	-3043
5047	5482	2102	3217	2945	1830
2804	5655	2163	3388	641	-584
6290	6416	2428	3437	3862	2853
35788	6895	2594	3554	33194	32234
7471	6821	2568	3610	4903	3861
39	6718	2533	3656	-2494	-3617
7494	6882	2589	3672	4905	3822
8451	6942	2610	3712	5841	4739
6003	6966	2618	3782	3385	2221
33685	7244	2714	3810	30971	29875

Mn Concentration ( $\mu\text{g g}^{-1}$ )				Error	
ICP	XRF	Empirical Calibration	GeoPIXE	XRF	GeoPIXE
6221	7273	2724	3937	3497	2284
6981	7527	2811	4034	4170	2947
1264	7256	2718	4039	-1454	-2775
6913	7638	2849	4172	4064	2741
3730	6897	2595	4198	1135	-468
8239	8008	2975	4208	5264	4031
8103	8025	2981	4384	5122	3719
3242	6845	2576	4528	666	-1286
7684	8365	3096	4556	4588	3128
10158	8702	3210	4687	6948	5471
9001	8752	3227	4744	5774	4257
6139	8541	3156	4761	2983	1378
66	8967	3300	4839	-3234	-4773
13907	9440	3459	5098	10448	8809
8187	9471	3470	5163	4717	3024
15190	9642	3527	5292	11663	9898
52399	10228	3723	5410	48676	46989
7072	9637	3525	5426	3547	1646
12192	10241	3727	5533	8465	6659
12188	10384	3775	5553	8413	6635
14319	10858	3933	5806	10386	8513
69	10806	3915	5807	-3846	-5738
17078	10831	3924	6094	13154	10984
17151	11420	4119	6290	13032	10861
22389	11670	4201	6328	18188	16061
21228	11635	4190	6343	17038	14885
23470	11726	4220	6391	19250	17079
22206	13038	4651	7219	17555	14987
8654	12730	4550	7263	4104	1391
19856	14418	5100	8039	14756	11817
14004	15115	5325	8194	8679	5810
22412	14960	5275	8337	17137	14075
14830	15621	5488	8492	9342	6338
15379	16247	5690	8798	9689	6581
11050	16451	5755	9386	5295	1664
26413	17001	5931	9495	20482	16918
14630	17450	6075	9629	8555	5001
23676	17622	6130	9980	17546	13696
15786	18734	6483	10330	9303	5456
15589	18283	6340	10332	9249	5257

<b>Mn Concentration (<math>\mu\text{g g}^{-1}</math>)</b>				<b>Error</b>	
<b>ICP</b>	<b>XRF</b>	<b>Empirical Calibration</b>	<b>GeoPIXE</b>	<b>XRF</b>	<b>GeoPIXE</b>
26691	19172	6622	10762	20069	15929
18394	20221	6953	11136	11441	7258
9749	18497	6408	11285	3341	-1536
21058	20162	6935	11319	14123	9739
22998	19626	6766	11670	16232	11328
21647	19506	6728	11801	14919	9846
26264	22099	7543	12955	18721	13309
24611	21804	7450	13438	17161	11173
22095	22035	7523	13706	14572	8389
9611	21784	7444	14308	2167	-4697
10499	25075	8469	15881	2030	-5382
15572	27107	9096	16598	6476	-1026
20422	29433	9809	16890	10613	3532
19363	29395	9797	18016	9566	1347
13613	29579	9853	18795	3760	-5182
Root mean square errors				6112.609	5290.945

**Table S3.** List of species with yttrium concentration detected, total number of specimens (N), specimens more than limit of detection (LOD), and concentrations (minimum–maximum [mean]).

Order	Taxon	N	> LOD	Yttrium concentration ( $\mu\text{g g}^{-1}$ )
Celastrales	<b>Celastraceae</b>	<b>1463</b>		
	<i>Denhamia oleaster</i>	132	1	310
Oxalidales	<b>Cunoniaceae</b>	<b>666</b>		
	<i>Gillbeea adenopetala</i>	47	1	105
	<i>Gillbeea whypallana</i>	14	1	180
Proteales	<b>Proteaceae</b>	<b>1841</b>		
	<i>Athertonia diversifolia</i>	64	1	190
	<i>Bleasdalea bleasdalei</i>	61	2	96–140 [120]
	<i>Cardwellia sublimis</i>	58	8	93–310 [170]
	<i>Helicia australasica</i>	34	21	93–1600 [440]
	<i>Helicia glabriflora</i>	32	14	71–1400 [590]
	<i>Helicia lamingtoniana</i>	2	1	98
	<i>Helicia lewisensis</i>	2	2	99–340 [210]
	<i>Helicia nortoniana</i>	10	5	140–920 [360]
	<i>Hicksbeachia pilosa</i>	7	1	78
	<i>Hicksbeachia pinnatifolia</i>	2	1	803
	<i>Hollandaea sayeriana</i>	8	2	240–503 [370]
	<i>Lasjia claudiensis</i>	9	4	110–190 [150]
	<i>Lasjia grandis</i>	5	4	72–140 [106]
	<i>Musgravea heterophylla</i>	20	1	530
<i>Xylomelum scottianum</i>	29	1	180	

**Table S4.** List of species with selenium concentration detected, total number of specimens (N), specimens more than limit of detection (LOD), and concentrations (minimum–maximum [mean]).

<b>Order</b>	<b>Taxon</b>	<b>N</b>	<b>&gt; LOD</b>	<b>Selenium concentration (<math>\mu\text{g g}^{-1}</math>)</b>
	<b>Proteaceae</b>	<b>1841</b>		
<b>Proteales</b>	<i>Austromuelleria trinervia</i>	45	12	84–308 [140]
	<i>Austromuelleria valida</i>	20	1	470
	<i>Bleasdalea bleasdalei</i>	61	1	110
	<i>Grevillea baileyana</i>	28	1	210

**Table S5.** List of species with >10,000 µg g<sup>-1</sup> Mn, total number of specimens (N), specimens less than limit of detection (LOD), and concentrations (minimum–maximum [mean]).

Order	Taxon	N	<LOD	Number of Hyperaccumulator specimens	Concentration (µg g <sup>-1</sup> )		Other studies
					This study	(Abubakari, Nkrumah, Erskine, <i>et al.</i> 2021; Abubakari, Nkrumah, Fernando, Brown, <i>et al.</i> 2021; Abubakari, Nkrumah, Fernando, Erskine, <i>et al.</i> 2021)	
Gentianales	<b>Apocynaceae</b>	372					
	<i>Alyxia magnifolia</i>	69	1	1	140–13,000 [2030]	Not Available	New
Celastrales	<b>Celastraceae</b>	146 3					
	<i>Denhamia bilocularis</i>	128	0	10	290–31,000 [4300]	470–15,300 [2300]	(Abubakari, Nkrumah, Erskine, <i>et al.</i> 2021)
	<i>Denhamia cunninghamii</i>	294	1	121	190–82,000 [10500]	290–32,000 [7150]	(Abubakari, Nkrumah, Erskine, <i>et al.</i> 2021)
	<i>Denhamia disperma</i>	160	9	1	150–11,000 [1900]	490–5400 [1440]	New
Myrtales	<b>Myrtaceae</b>	636					
	<i>Gossia acmenoides</i>	48	0	4	430–12,000 [3600]	371–7040 [ 2150]	New
	<i>Gossia bamagensis</i>	15	1	11	3400–48,000	134–22,900[11800]	(Fernando et al. 2009; Abubakari et al.

Order	Taxon	N	<LOD	Number of Hyperaccumulator	Concentration ( $\mu\text{g g}^{-1}$ )		Other studies
					[22,000]		2021b)
	<i>Gossia bidwillii</i>	139	0	78	550–45,000 [12500]	880–20,900 [6800]	(Bidwell et al. 2002; Abubakari et al. 2021b)
	<i>Gossia dallachiana</i>	41	0	19	1200– 31,000 [9800]	890–20,400 [5800]	(Abubakari, Nkrumah, Fernando, Brown, <i>et al.</i> 2021)
	<i>Gossia floribunda</i>	44	0	2	330–15,000 [4070]	277–7210 [2330]	New
	<i>Gossia fragrantissima</i>	10	0	8	5800– 24,000 [15,000]	3600–13,200 [7800]	(Fernando et al. 2009; Abubakari et al. 2021b)
	<i>Gossia gonoclada</i>	22	0	11	170–22,000 [10300]	460–10,800 [5600]	(Fernando et al. 2009; Abubakari et al. 2021b)
	<i>Gossia grayi</i>	21	0	2	630–11,000 [4600]	550–5200 [2500]	New
	<i>Gossia hillii</i>	22	0	1	230–23,000 [3300]	500–13,000	(Abubakari, Nkrumah, Fernando, Brown, <i>et al.</i> 2021)
	<i>Gossia lucida</i>	18	0	4	780–16,000 [6900]	570–8500 [3700]	New

Order	Taxon	N	<LOD	Number of Hyperaccumulator	Concentration ( $\mu\text{g g}^{-1}$ )		Other studies
	<i>Gossia myrsinocarpa</i>	44	1	1	530–12,000 [3200]	180–1800 [730]	New
	<i>Gossia pubiflora</i>	25	0	12	1500–33,000 [12,000]	1030–16,000 [6600]	(Abubakari, Nkrumah, Fernando, Brown, <i>et al.</i> 2021)
	<i>Gossia retusa</i>	21	2	3	203–15,000 [4200]	28–7200 [2010]	New
	<i>Gossia sankowskyorum</i>	33	1	14	400–40,000 [10,300]	480–12,000 [5200]	(Abubakari, Nkrumah, Fernando, Brown, <i>et al.</i> 2021)
	<i>Gossia shepherdii</i>	43	1	14	450–30,300 [8400]	470–15,000 [4600]	(Abubakari, Nkrumah, Fernando, Brown, <i>et al.</i> 2021)
Malpighiales	<b>Phyllanthaceae</b>	633					
	<i>Glochidion sumatranum</i>	5	1	1	185–11,000 [3300]	Not Available	New
Proteales	<b>Proteaceae</b>	235 1					
	<i>Helicia australasica</i>	34	8	1	134–12,000 [1400]	Not Available	New
	<i>Helicia glabriflora</i>	32	3	1	206–13,000 [22-0]	Not Available	New

Order	Taxon	N	<LOD	Number of Hyperaccumulator	Concentration ( $\mu\text{g g}^{-1}$ )		Other studies
	<i>Lomatia arborescens</i>	8	0	1	190–10,000 [4400]		New
	<i>Macadamia integrifolia</i>	16	1	2	190–15,000 [4100]	190–8500 [3200]	New
	<i>Macadamia ternifolia</i>	21	0	3	210–18,000 [4600]	210–9600 [3000]	New
	<i>Sphalmium racemosum</i>	39	33	1	130–10,400 [2900]	Not Available	New